A&A 385, 479–487 (2002)
DOI: 10.1051/0004-6361:20020153

Astronomy & Astrophysics

Spectral variability of luminous early type stars

II. Supergiant α Camelopardalis

N. Markova⋆

Institute of Astronomy and Isaac Newton Institute of Chile Bulgarian Branch, Bulgarian National Astronomical Observatory, PO Box 136, 4700 Smoljan, Bulgaria

Received 7 September 2001 / Accepted 15 January 2002

Abstract. Time-series of Hα spectra with relatively high resolution in wavelength ($R = \lambda/\delta\lambda$ of 15 000 to 22 000) and time ($\Delta t = 1^{\rm d}$) of the late-type O supergiant α Cam are analysed in terms of line-profile variability (lpv). The spectra cover an interval of one year, from February 1998 to February 1999. The analysis provides clear evidence of a continuous deep-seated wind activity traced by variations in the Hα emission and He I λ6678.15 absorption lines. The observations indicate that the wind is not smooth but perturbed, starting from its base up to velocities of ∼500 km s^{-1}. The character of the medium-term (days) variations found in Hα changes between epochs, and appears to require an explanation involving different kinds of wind perturbations. In particular, we found that in June and July 1998 as well as in February 1999 the lpv of Hα was dominated by low-amplitude ($\leq\pm$10%) variations in line flux which usually occupy the central part of the profile symmetrically with respect to the line center while in December 1998 and January 1999 the variations were organised in two wave-like modulations that run from "red" to "blue" and back to "red" within the profile (between ±300 km s^{-1}), being most of the time in antiphase. The timescale of variation, revealed via Fourier analysis, is respectively ∼7 and ∼10 days. Significant variations in emission equivalent width (up to 35%), closely linked to those in the line profile, are also noted. Short-term (3 to 4 days), low-amplitude ($\leq$22%) variation in mass loss rate which recurs on a timescale of ∼7 days giving rise to the formation of outward accelerating consecutive shells or/and blobs was suggested to explain the lpv of Hα in June–July 1998 and in February 1999. Whereas the variability pattern observed in December–January 1999 seems to be qualitatively consistent with a model involving two rotationally-modulated wind perturbations, one of enhanced density and another of reduced density with respect to the mean, which are not symmetric about the center of the star. Strange-mode oscillations or radial fundamental pulsation are discussed as possible mechanisms generating the established wind variability.

Key words. stars: oscillations – stars: mass loss – stars: individual: α Cam

1. Introduction

O-star winds are known to be highly variable. The most prominent signatures of this variability are Discrete Absorption Components which migrate from red to blue through unsaturated P Cygni profiles of UV resonance lines. Observations indicate that stellar rotation plays a dominant role in setting the recurrence timescale of the DACs variability (Prinja 1988; Kaper 1999). Because of their ubiquity, DACs are believed to be a fundamental property of O-star winds (Howarth & Prinja 1989). Besides variations in UV resonance lines, several other aspects of wind activity have been observed. Among these are variability in X-ray (Berghofer et al. 1996; Berghofer 1999), optical and radio wavebands and in polarisation. Variations in optical emission lines of strong H and He transitions are also detected (Ebbets 1982; Prinja et al. 1996; Kaper et al. 1997; Rauw & Vreux 1998; de Jong et al. 2001; Prinja et al. 2001).

On the other hand, absorption line-profile variability (lpv) seems to be commonplace among O stars (Baade 1992; Fullerton et al. 1996). It seems that stellar pulsation is responsible for this variability (Fullerton et al. 1996; de Jong et al. 1999). The coexistence of photospheric and wind variability in hot luminous stars and the rough similarity of their timescales – typically of a few hours to weeks – suggests that the two phenomena might be related in some way. The search for such a relationship is known as a search for "a photospheric connection" (Reid & Howarth 1996).

The supergiant α Cam (O9.5 Ia) is a runaway star that is supposed to be a member of the young open cluster NGC 1502 (d = 1.2 kpc). The fundamental stellar and wind parameters we have adopted are listed in Table 1.

⋆ e-mail: rozhen@mbox.digsys.bg

Table 1. Stellar parameters of α Cam.

Quantity	Value	Source
Spectral Type	O9.5 Ia	LDF (1992)*
V	4.29	LDF (1992)
$B-V$	+0.03	LDF (1992)
M_V	−7.1	LDF (1992)
$T_{\rm eff}$[K]	30 000	Puls et al. (1996)
$\log L/L_\odot$	5.79	Puls et al. (1996)
$R/R_\odot$	29	Puls et al. (1996)
$\log M/M_\odot$	1.49	Puls et al. (1996)
$\log g$	3.00	Puls et al. (1996)
$V_{\rm sys}$ [km s^{-1}]	6 to 18	various sources
$v \sin i$	80	Puls et al. (1996)
$V_{\rm inf}$ [km s^{-1}]	1 550	Puls et al. (1996)
$\log \dot{M}$ [$M_\odot$ yr^{-1}]	−5.2	Puls et al. (1996)
β	1.1	Puls et al. (1996)

* LDF corresponds to Lennon et al. (1992).

The systemic velocity of the star is not well fixed – the values found in the literature range from 6 to 18 km s^{-1} – and for this reason the stellar rest frame is not used as a reference for the radial velocity determinations presented hereafter.

Wind variability in α Cam has been recognised as night-by-night variations in Hα (Ebbets 1982; Kaper et al. 1997). Changes in the strong and saturated UV resonance lines of Si IV, C IV and N V were reported by Lamers et al. (1988) but were not confirmed by Prinja & Howarth (1986) and Kaper et al. (1996). Absorption line-profile variability was detected by Zeinalov & Musaev (1986) and by Fullerton et al. (1996). The timescales of the wind and photospheric variabilities are poorly determined but appear to be of a few days. The star has not been analysed in terms of the "photospheric connection".

The main objective of our study is to investigate the co-variability of Hα emission and He I λ6678 absorption in α Cam. This way we hope to gain a better understanding of the nature and origin of variability of the star. The observations and reductions are described in Sect. 2. In Sect. 3 the temporal behaviour of Hα and He I λ6678 is examined using state of the art techniques of time-series analysis, such as the Temporal Variance Spectrum (TVS) and the two dimensional Discrete Fourier Transform (2d-DFT). Some line-parameters such as radial velocity and equivalent width are measured and analysed in terms of time-variability. The obtained results are discussed in Sect. 4 where a possible interpretation of the results is given.

2. Observations and data reduction

The observations presented here have been obtained within an on-going program studying wind variability of luminous early-type stars. We used the coude spectrograph of the 2 m RCC telescope at the National Astronomical Observatory, Bulgaria. The project was started in 1997 with an ELECTRON CCD with 520 × 580 pixels of 22 × 24 μ as detector. Beginning in Autumn of 1998, we used a PHOTOMETRICS CCD with a pixel area of 1024 × 1024 and a pixel size of 24 μ. With the former configuration, about 115 Å with resolution R = 15 000 can be observed in one exposure, while with the latter one the spectrum coverage is about 200 Å with the same resolution of 15 000. In April 1998 a few spectra with R = 15 000 and a spectral length of 72 Å were obtained using an SBIG (Santa Barbara Instrument Group) ST6 Thomson CCD with an area of 375 × 242 and a pixel size of 23 × 27 μ.

Our data sample consists of 65 spectra of α Cam, in the wavelength domain of Hα, obtained between February 1998 and February 1999. The distribution of the observations in time is given in Tables 2 and 3. In both tables Col. 2 gives the Heliocentric Julian Date; Col. 3 in

Table 2. Journal of observations.

Date	HJD	$R=\lambda/\delta\lambda$	Coverage	S/N	W_λ(Hα)
	2 450 000+		in Å		in Å
1998/02/08	853.398	22 000	57	183	−3.2
1998/02/10	855.166	15 000	114	228	−2.29
1998/03/06	879.389	15 000	114	393	−1.89
1998/03/07	880.399	15 000	114	187	−1.94
1998/03/08	881.423	15 000	114	138	−2.67
1998/04/13	917.306	15 000	72	179	−3.04
1998/04/14	918.492	15 000	72	91	−2.98
1998/05/07	941.268	22 000	57	87	−1.79
1998/05/19	953.250	15 000	114	52	−1.83
1998/06/03	968.254	15 000	114	275	−1.72
1998/06/04	969.248	15 000	115	185	−2.67
1998/06/05	970.255	15 000	115	191	−2.76
1998/06/06	971.238	15 000	115	161	−2.63
1998/06/07	972.259	15 000	115	323	−1.48
1998/06/08	973.253	15 000	114	75	−2.24
1998/06/09	974.586	22 000	57	174	−1.77
1998/06/10	975.584	22 000	57	172	−1.78
1998/06/11	976.260	22 000	57	162	−2.14
1998/06/11	976.586	22 000	57	69	−2.82
1998/06/14	979.590	22 000	57	122	−2.61
1998/06/16	981.261	15 000	114	163	−1.68
1998/06/16	981.574	15 000	115	215	−1.63
1998/06/17	982.257	15 000	114	485	−2.38
1998/06/17	982.572	15 000	114	176	−2.68
1998/07/03	998.265	15 000	114	117	−2.45
1998/07/03	998.370	15 000	114	148	−2.38
1998/07/03	998.445	15 000	114	219	−2.78
1998/07/03	998.579	15 000	114	278	−2.80
1998/07/06	1001.574	15 000	114	171	−3.08
1998/07/07	1002.301	15 000	114	207	−2.29
1998/07/07	1002.573	15 000	114	121	−2.70
1998/07/10	1005.599	15 000	114	294	−2.11
1998/07/11	1006.573	15 000	114	196	−2.43
1998/07/12	1007.565	15 000	114	186	−2.89
1998/07/13	1008.584	15 000	114	180	−2.92
1998/07/14	1009.561	22 000	58	118	−2.86
1998/10/04	1091.639	15 000	204	543	−1.99
1998/10/09	1096.628	15 000	204	367	−2.62
1998/11/02	1120.452	22 000	102	246	−2.68
1998/11/02	1120.628	22 000	102	249	−2.60

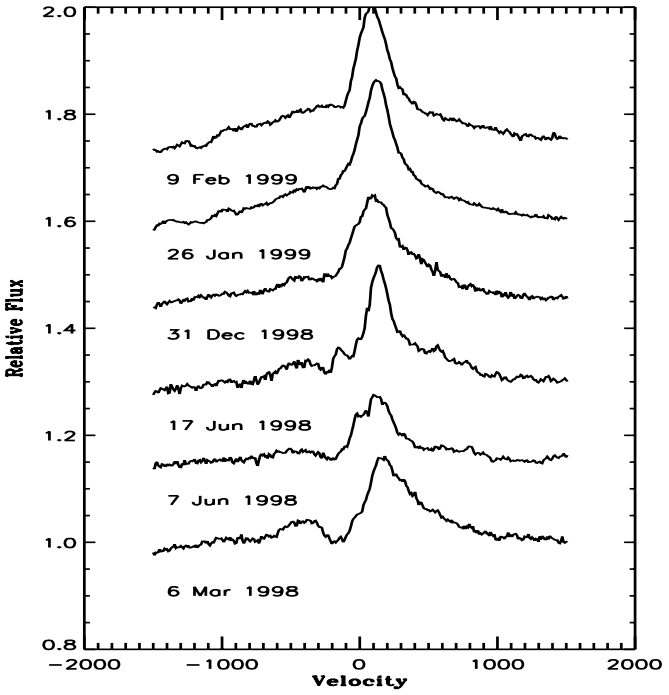

Fig. 1. Examples of differently shaped Hα profiles of α Cam obtained during the observations. The spectra are shifted vertically to ensure better visibility. The position of the He II λ6560.2 absorption trough is expected to be at $\sim$−120 km s^{-1}

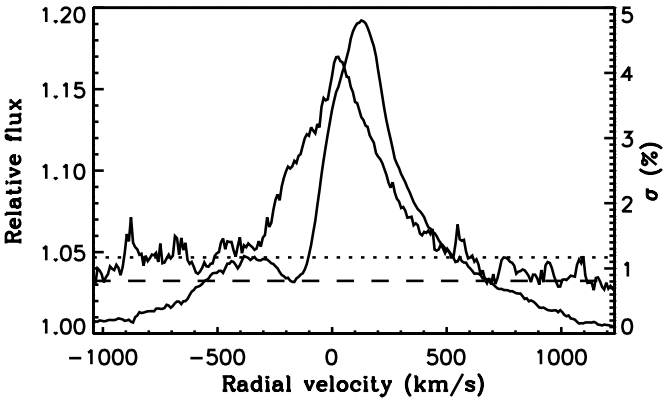

Fig. 2. The average Hα profile (thick line) and the *rms* deviations for the entire data set as a function of velocity across the line. The dashed line indicates the level of deviations in the continuum (σ_C). The threshold for variability ($p = 1\%$) is indicated by a dotted line.

Table 2 records the spectral resolution, $R = \lambda/\delta\lambda$ (This information is not given in Table 3 because all spectra listed in this table have the same resolution of 15 000.); Cols. 4 (Table 2) and 3 (Table 3) list the wavelength span recorded, $\Delta\lambda$; Col. 5 (Table 2) and 4 (Table 3) – the S/N ratio. We followed a standard procedure for data reduction including: bias subtraction, flat-fielding, cosmic ray hits removal, wavelength calibration and correction for heliocentric radial velocity. The spectra were normalised by a polynomial fit to the continuum, specified by carefully selected continuum windows, and rebinned to a step

Table 3. Journal of observations – continued.

Date	HJD 2 450 000+	Coverage in Å	S/N	W_λ(Hα) in Å	V_r(He I λ6678) in km s^{-1}
1998/12/30	1178.194	120	444	−2.29	0
1998/12/30	1178.449	120	302	−2.40	0
1998/12/30	1178.689	120	295	−2.44	–1
1998/12/31	1179.161	204	260	−2.33	22
1998/12/31	1179.473	204	366	−2.41	15
1998/12/31	1179.689	204	379	−2.61	15
1999/01/02	1181.356	120	121	−2.69	—
1999/01/05	1184.420	204	403	−2.41	0
1999/01/05	1184.675	204	343	−2.44	26
1999/01/06	1185.165	204	240	−2.31	7
1999/01/06	1185.511	204	198	−2.62	0
1999/01/06	1185.695	204	329	−2.88	13
1999/01/07	1186.163	204	669	−2.67	7
1999/01/07	1186.483	204	309	−2.73	0
1999/01/07	1186.634	204	368	−2.84	0
1999/01/07	1186.688	204	223	−2.65	–7
1999/01/08	1187.433	204	161	−2.58	13
1999/01/09	1188.313	204	417	−2.30	8
1999/01/09	1188.628	204	234	−2.70	1
1999/01/10	1189.153	204	446	−2.86	31
1999/01/26	1205.173	204	325	−2.91	—
1999/01/26	1205.620	204	395	−3.37	—
1999/02/05	1215.179	204	420	−2.45	—
1999/02/07	1217.454	204	393	−3.11	—
1999/02/09	1219.175	204	396	−3.20	—

of 0.2 Å per pixel. The atmospheric water vapour lines were removed by dividing each spectrum of α Cam with a specially constructed "telluric spectrum". All steps in the reduction procedure were performed using a series of modules written in IDL. More information about the observations and the reduction procedure can be found in Markova & Valchev (2000).

3. Results

3.1. Variability of Hα

During our observations the Hα line of α Cam displayed large variations in shape from a P Cygni-like profile to pure asymmetric or double-peaked emission. Examples of representative profiles are shown in Fig. 1. Close inspection of the data obtained over the entire time interval covered by the observations revealed that the profiles are quite similar, both in shape and intensity, to those obtained by Ebbets (1982) and by Kaper et al. (1997). This result indicates that wind variations on a timescale of years do not seem to be important in α Cam.

To quantify the observed variations we computed the rms deviations of the normalised Hα profiles with respect to the mean for the entire data set line profile as a function of wavelength, σ_λ, assuming that the noise is dominated by photon noise and is nearly the same for each spectrum in the time series. This approach, first used by Prinja et al. (1996), represents a good approximation of the rigorous Temporal Variance Spectrum (TVS, Fullerton et al. (1996). The averaged Hα profile and the rms deviations as

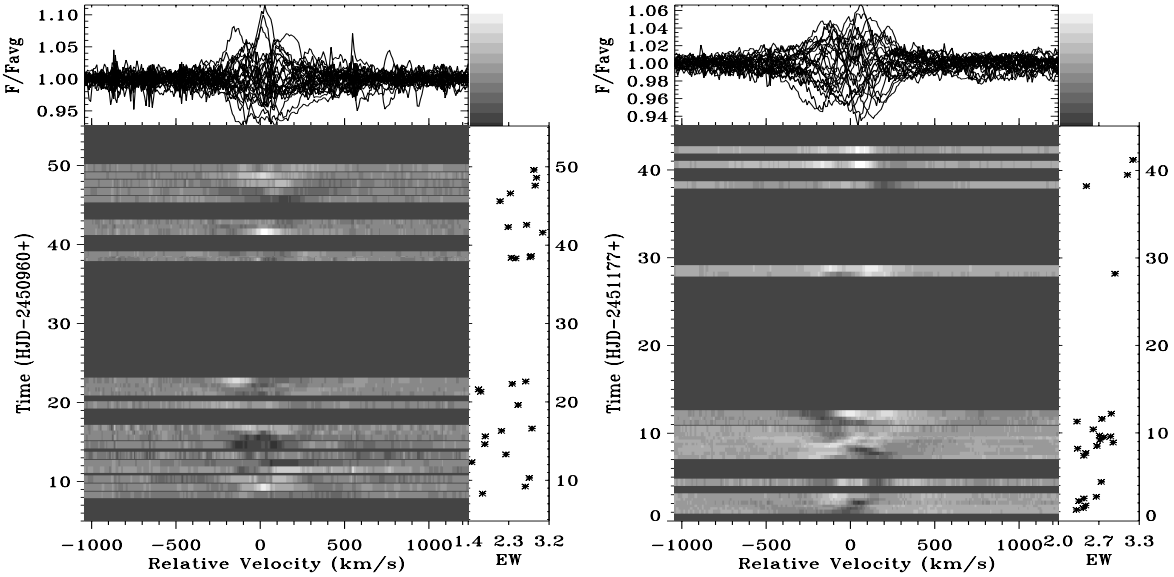

Fig. 3. Dynamic quotient spectra of Hα in June–July 1998 (left panel) and in December–February 1999 (right panel). The zero-point in velocity is set to the laboratory wavelength of the line. The top panels show an overplot of all profiles from the relevant time series. The gray-scale bar on the right of each plot shows the intensity scaling. The panel on the right-hand side of each image shows the equivalent width of the line (in Å) as a function of time.

a function of velocity across the profile are shown in Fig. 2. The mean profile consists of well-developed P Cygni-like core with a peak emission at $\sim$+110 km s^{-1} with respect to $V_{\rm sys}$ (if $V_{\rm sys}$ = +18 km s^{-1}) and an absorption dip at $\sim$−192 km s^{-1}. The P Cygni core is superimposed on broad emission wings ($\sim\pm$1000 km s^{-1}). If the total emission flux is estimated by twice the equivalent width measured redward from $V_{\rm sys}$, then the observed reduction in flux blueward of $V_{\rm sys}$ ($\sim$27%) is probably too large to be explained by He II λ6560 absorption. This suggests that most of the blueward dip is formed by Hα absorption in the stellar wind. The TVS presented in Fig. 2 indicates that significant lpv occurs in the inner part of the wind ($V_{\rm r} \leq 0.32\ V_{\rm inf}$) while the outer wind layers, where the emission wings presumably originate, are marginally variable, in agreement with the finding of Ebbets (1982).

The two longest Hα time-series, from June−July 1998 and December 1998−February 1999, are presented in Fig. 3 in the form of two-dimensional gray-scale images. The contrast in these images has been enhanced by dividing each member of the time-series by the respective mean spectrum (the so-called "dynamic quotient spectrum"). Hence, regions and times of excess emission with respect to the mean appear brighter, while darker regions indicate intervals when the local flux was smaller than its mean value. The plots on the right-hand side of the images show the equivalent width (W_λ) of the line, measured by line-flux integration between 6542 and 6588 Å, as a function of time. The internal precision of individual W_λ determinations, evaluated by means of the formula provided by Chalabaev & Maillard (1983), equals $\sim$0.29 Å and $\sim$0.15 Å for Hα profiles obtained before October 1998 and afterwards. The results presented in Fig. 3 clearly indicate that the Hα profile is continuously variable over the whole time interval covered by the observations. The variations are more systematic than erratic but the pattern of variability changes from one observational epoch to another.

In June and July, for example, episodes of enhanced emission alternate with those of reduced emission. The episodes seem to recur on timescales of approximately 7 days. Substantial variations occur predominantly in the central part of the profile, almost symmetrically with respect to the stellar rest frame. The observed lpv is accompanied by variations in W_λ in sense that episodes of enhanced/reduced central emission conform to larger/smaller emission equivalent width. Notice the sudden appearance of the blue-shifted enhanced emission at $\sim$–150 km s^{-1} on T = 22 days.

The December−February quotient spectrum (right-hand panel of Fig. 3) reveals another variability pattern: two waves, one of enhanced emission and another of reduced emission/enhanced absorption, run from "red" to "blue" and back to "red" within the profile (between $\pm$300 km s^{-1}). From T = 0 to T = 5 days these waves appear to be in phase whereas from T = 7 to T = 11 days they are almost in antiphase. In addition to the wave-like variability an episode of enhanced blue-shifted absorption is clearly noted (T = 11 to T = 12 days). The absorption moves from about –50 to about –200 km s^{-1} with a mean acceleration of $\sim$0.0017 km s^{-2}. The event has been accompanied by strong increase in emission spread to $\sim$+500 km s^{-1}. Notice that the W_λ of the line, presented on the right-hand panel of the image, reaches its maximum values when the wave of enhanced emission passes the systemic velocity of the star. The observed lpv implies deviation from spherical symmetry and presence

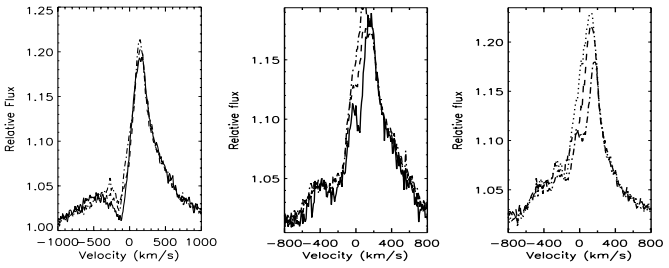

Fig. 4. Examples of short-term lpv of Hα. Profiles obtained within one night are overploted to enhance the significance of the observed variations. From left to right the corresponding dates of observations are: July 7, 1989; December 31, 1989 and January 6, 1999

of large-scale, time-dependent density perturbations in a wind that might be rotationally modulated.

Although scanty the February observations ($T = \geq 38$ days) clearly indicate that the wave-like phenomenon observed in December−January is no longer at work. The episode of enhanced emission ($T =$ 40 to 43 days) is obviously reminiscent of those observed in June and July. Notice the red-shifted region of reduced emission seen on $T = 38$ days. The results imply that the star had likely returned to the kind of behaviour it showed in June and July, which seems to be its "normal" state.

Ebbets (1982) and Kaper et al. (1997) noted only minor changes in the Hα profile of α Cam on a timescale of hours. Our observations, however, indicate that this is not the case all the time. For example, the lpv detected within one night in July 1989 (Fig. 4, left panel) was indeed marginal but in December−January (Fig. 4, middle and right panels) they were substantial. It must be noted however that whenever intensive observations over consecutive nights are available it can be seen that the short-term variations are consistent with the night-to-night variability. This result indicates that the short-term variability of Hα is due to the same phenomenon that causes the medium-term, i.e. night-to-night, variability.

Finally, it is interesting to note that the full range in observed emission equivalent width corresponds to a 22% variation in mass loss rate for a model based on a spherically symmetric, smooth wind outflow. This estimate was obtained using a scaling relation between the mass loss rate derived by Hα and the stellar and wind parameters (Puls et al. 1996, Eq. (42)). To derive the net wind emission from the observed equivalent widths of Hα the latter were corrected for the effect of the underlying photospheric absorption (=2.96 Å) as well as for the blending effect of He II λ6560 (=1.0 Å). The numbers in brackets are taken from Puls et al. (1996). The equivalent width measurements for the Hα emission are given in Col. 6 of Table 2 and Col. 5 of Table 3.

3.2. Line-profile variations in the He I λ6678.15 absorption line. Comparison with variations in Hα

The TVS of He I λ6678, shown on the right top panel of Fig. 6, indicates that significant variability in the line occurs over a velocity range of $\sim$400 km s^{-1}, that is a factor of 2 to 3 larger than the expected width of a photospheric line with no other broadening than stellar rotation ($2\ v \sin i = 160$ km s^{-1}). This finding indicates that the variability of He I λ6678 is at least partially connected to the wind. The double-peaked morphology of the TVS is indicative of radial velocity variability in the core of the line. The more intensive blue peak suggests existence of lpv that operates only at higher negative velocities. The extended red wing of the distribution might imply that the nearby He II λ6683 line is variable too, though at a much lower level of significance than that He I λ6678.

In Fig. 5 the lpv of Hα over the December−January run (from December 30, 1998 to January 10, 1999) is compared to that of He I λ6678.15 and He II λ6683.2. The image portion represents the corresponding dynamic quotient spectrum. The zero point in velocity for the He I+He II line complex is set at the wavelength of He I λ6678.15. Within this velocity scaling the expected position of He II λ6683 is at +227 km s^{-1}. The dynamic quotient spectrum of the He I+He II complex (right panel) gives clear evidence for systematic line-flux variations in the He I λ6678 profile (within $\pm$4% in continuum units). No indication for such variations in the He II λ6683 profile is noticed. The He I λ6678 variations are almost symmetric with respect to the line center. The pattern of variability is reminiscent of that of Hα but some differences are still noted. For example, the variations extend to lower velocities, $\sim\pm$200 km s^{-1}. Also the episode of enhanced blue-shifted absorption seen in Hα during the last few days of the run is not observed in He I λ6678. No clear evidence for a time lag between the variations in the two lines is seen. These results suggest that first, the He II λ6683 line is more likely of "pure" photospheric origin and second, the He I λ6678 absorption line is partially formed in the wind, as suggested by the analysis of the TVS plot, and its behaviour is strongly affected by the same processes that determine the variability of Hα.

That the He I λ6678 absorption line is not of "pure" photospheric origin is also apparent from its mean radial velocity which equals $+7.9 \pm 10.4$ km s^{-1}. This value is lower (by $\sim$27 km s^{-1}) than the highest positive velocities measured in the optical spectrum of α Cam (Gies, private communication) suggesting that the He I λ6678 line is likely formed in layers of the atmosphere that are already flowing outward with respect to the static photospheric layers. Our radial velocity measurements were made by fitting a parabola to the lower part of the profile and using the minimum of the fit to represent the position of the line. This method seems to be appropriate for He I λ6678 since the line is deep, narrow and free from blending with the nearby He II λ6683. The measurements, listed in the last column of Table 3, show that the He I λ6678 absorption

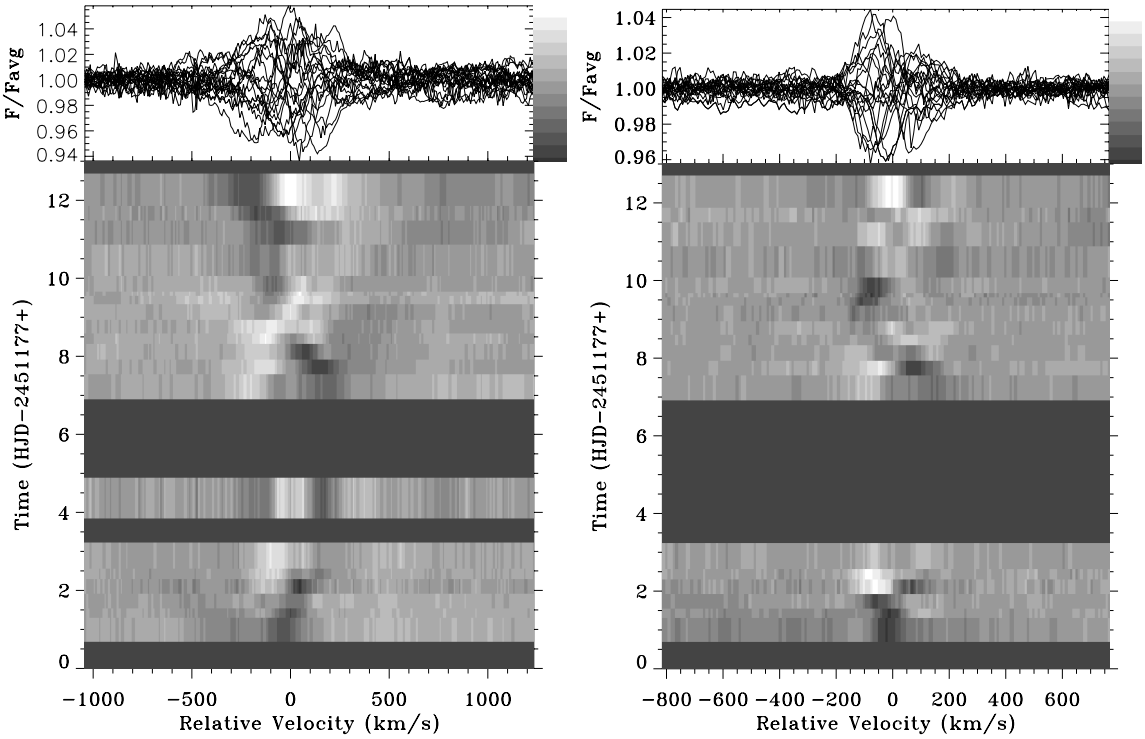

Fig. 5. Dynamic quotient spectra of Hα (left panel) and the He I λ6678 and He II λ6683 lines (right panel) in December 1998−January 1999. The zero-point in velocity is set at the laboratory wavelength of Hα and He I λ6678.15. Darker shadings in the image denote regions and times where the profile has a lower intensity than its time-averaged value. Panels on the top show an overplot of all profiles (in difference flux) from the relevant time series. The gray-scale bar on the right of each plot shows the intensity scaling.

line is radial-velocity variable, in agreement with the result derived from the analysis of the TVS. The variations are systematic and occur on a timescale of 3 to 4 days. The amplitude of variation is ± 20 km s^{-1}, i.e. a factor of 5 larger than the precision of individual radial-velocity determinations.

3.3. Searching for periodic variability

A period analysis, based on the 2-d Discrete Fourier Transform and the iterative CLEAN algorithm (Roberts et al. 1987), was performed for the Hα profiles taken in June−July 1998 as well as for the Hα and He I λ6678 profiles obtained between December 30 and January 10, 1999. The resulting power spectra are shown as gray-scale representations in Fig. 6. Panels on the right of each image show the power summed over the profile as a function of frequency. The mean spectrum of the time-series and the rms deviations with respect to the mean are plotted in the upper panels. The June-July periodogram of Hα (left-hand panel) shows maximum power at 0.859 ± 0.022 ($P = 1.16$ days) and at 0.143 ± 0.020 d^{-1} ($P = 6.99$ days). Due to the time-resolution of the relevant observations we consider the 1.16 days signal to be inconclusive. Concerning the $\sim$7 days variation, we suggest, based on the similarity of the relevant timescales, that this variation refers to the recurrent appearance of episodes of enhanced/reduced emission in the line (see the left-hand panel of Fig. 3).

The images referring to the December−January time-series (middle panel for Hα and right-hand panel for He I λ6678) provide suggestive evidence for periodic variability at least at two frequencies, with a reasonable degree of correspondence between the two lines. In decreasing order of summed power, the dominant frequencies are: 0.339 ± 0.025 d^{-1}, 0.175 ± 0.022 d^{-1} in Hα and 0.225 ± 0.023 d^{-1} and 0.354 ± 0.022 d^{-1} in He I λ6678. (We derived the frequencies of maximum power by means of Gaussian fits. The errors were derived from the width of the peak.) The mean of these frequencies corresponds to $P_1 = 2.89$ and $P_2 = 5.00$ days (with an uncertainty of $\leq$10%). The former period operates in velocity ranges [0, +200] and [−200, +200] in Hα and He I λ6678, respectively while the latter dominates variations in the velocity range [0, −200] within each line. The 3-days variation seems to reflect cyclic variations in equivalent width (Hα) and in radial velocity (He I λ6678) while the 5-days variation is more likely connected with the wave-like modulations revealed via the dynamic quotient spectra (see Sect. 3.2). The actual timescale of this variation may be $\sim$10 days since a half but not a full cycle was observed. This suggestion seems to be supported by the result that the periodogram of Hα shows significant power at frequency of 0.095 ± 0.024 d^{-1} ($P = 10.5$ days). The reality of this variation however is difficult to assess since

its frequency is rather close to $\nu_{\rm min} = 0.083$ d^{-1}, i.e. the shortest frequency sampled in this data set.

Finally, note that because of our restricted time sampling, we prefer to refer the results above as timescales of variability rather than strict periodicities.

4. Discussion and conclusions

The present analysis provides clear evidence of continuous deep seated wind activity in α Cam, recognised as variations in Hα and He I λ6678. The variations are systematic and occur on a timescale $\sim$7 days in June–July 1998 and $\sim$10 days in December–January 1999.

Gabler et al. (1989) and Scuderi et al. (1992) argued that O-star winds are optically thin in Hα. However, Puls et al. (1996) demonstrated, based on a detailed analytical discussion of Hα line formation in O-star winds, that the optically thin approach is not absolutely correct and leads to significant systematic error. Indeed, Hα observations of a number of O-type stars revealed strong departures from a pure wind emission profile (Prinja et al. 1996; Rauw et al 2001). Our observations also indicate that the wind of α Cam is not, at least not always, optically thin in Hα. In particular, we found that in some occasions the opacity in the inner part of the wind can become so large that a detailed balancing between photoionization out of, and recombination back into the ground state is reached and Hα starts to behave as a scattering line. In case the opacity variations are due to changes in number density of the wind and if a spherically symmetric smooth stellar wind is to be considered than the extreme variations in Hα would require 22% alterations in mass loss rate. However, the observations indicate that the long-term behaviour of Hα is rather complex and does not always conform to mass loss variations in a spherically symmetric wind.

4.1. Towards a possible interpretation of the wind variability

It is nowadays widely accepted that all O and many B stars show cyclical variability in their wind. In some cases the variations have been traced from close to the stellar surface (Hα) to far out in the wind (DAC's in the UV). The timescale of the cyclic variability seems to be closely related to the stellar rotation period. This phenomenon may result from either large-scale spiral-shaped structures rooted in and corotating with the photosphere, the so-called CIRs model, firstly proposed by Mullan (1984) and additionally worked out by Cranmer & Owocki (1996), or a tilted confined corotating wind (Kaper et al. 1997; Stahl et al. 1996; Rauw et al 2001; de Jong et al. 2001).

The Hα observations of α Cam in June–July 1998 and in February 1999 did not give evidence of either large-scale asymmetries or periodic modulations in the wind of the star. Conversely, the observations appear to be widely consistent, at least qualitatively, with the idea of short-term, low-amplitude variations in mass loss rate which cause the formation of large-scale density perturbations in the wind. Indeed, the sort of the observed lpv suggests that the inner wind of the star is not smooth but perturbed. Since variations in W_λ relevant to those in the line profile were also detected we suggest that the wind perturbations are more likely caused by changes in mass loss rate, $\dot{M}$. If this interpretation is correct, then it implies a 19% variation in $\dot{M}$ in order to account for the extreme variation observed in the Hα emission between June 3 and July 14. Unfortunately, it seems not possible to judge, based on the available observations, what the morphology of the wind structure is. On the one hand, the perturbations should be large and should have significant azimuthal extents so as to be able to significantly modify the profile over an extended velocity range simultaneously (e.g. shells, large blobs). The result that the enhanced emission produced by the perturbations usually occupy the central part of the Hα profile symmetrically with respect to the line center and especially the finding that this event recurs on a timescale of $\sim$7 days seem to argue in favour of consecutive spherically symmetric shells. However, the appearance of the blue-shifted enhanced emission on HJD 2450982 (T = 22 days, Fig. 3, left panel) and of the red-shifted reduced emission on HJD 24501215 (T = 38 days, Fig. 3 left panel) clearly indicates that deviation from spherical symmetry in the form of spatially localised, smaller-scale density perturbations can also occur. Thus we conclude that over the June–July 1998 observations α Cam has more likely experienced a short-term (3 to 4 days), low-amplitude ($\leq$19%) variation in $\dot{M}$ which seems to recur on a timescale of $\sim$7 days, giving rise to the formation of outward accelerating consecutive shells or/and blobs. Since the behaviour of the star in February 1999 closely resembles that in June–July 1998 we furthermore suggest that this kind of behaviour is more likely the "normal" (i.e. more frequently observed) behaviour of α Cam. The presence of outward accelerating shells or blobs caused by 10 to 30% variations in $\dot{M}$ was suggested by de Jager et al. (1979) and Lamers et al. (1988) to explain the daily changes in the high-velocity part of the UV line profiles of α Cam. The quoted limits for $\dot{M}$ variations in the UV as well as the timescale on which these variations occur ($\sim$3 days) are in good agreement with the estimates derived via Hα (present study) suggesting that the same phenomenon is more likely responsible for the lpv observed in the two wavelength regions.

It may be that the deep-seated wind variability of α Cam in December 1998–January 1999 is due to the rotational modulation of a perturbed stellar wind. The timescale of this variability (=10.5 days) falls just between the lower (=4.9 days) and upper (=18.3 days) limits for the rotational period of the star determined by $V \sin i$ and the adopted stellar parameters. This result suggests that stellar rotation may play a role in setting the timescale of the established phenomenon. On the other hand, Harries (2000) found, based on line-profile simulations, that a corotating spiral density enhancement produces a S-wave-like pattern as a function of rotational phase. A direct comparison of the image shown in the

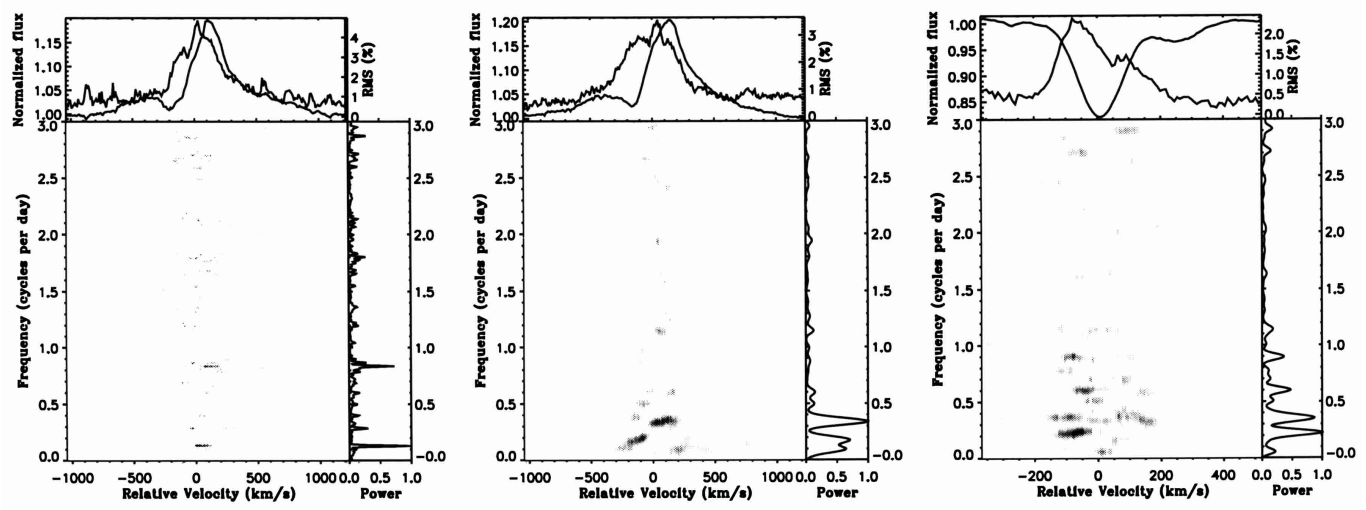

Fig. 6. Temporal Variance Spectrum and 2d-Fourier Transform created from the Hα time-series taken in June−July 1998 (left panel) and in December−January 1999 (middle panel). The right-hand panel shows the TVS and the 2DFT of He I λ6678 in December−January 1999. The image portion of each panel displays the power as a function of velocity and frequency. The power summed over the profile is shown to the right of each image.

right-hand panel of our Fig. 3 with Fig. 4 in Harries (2000) shows that the wave-like "bright" modulation observed by us is similar to the pattern he derived. The agreement is not only qualitative but also quantitative since the observed upper limit for variations of the individual Hα profiles from the mean ($\sim$6%) is practically equal to that predicted by the model ($\sim$5%). Furthermore, the shape of the equivalent curve of Hα with its steep increase and slower decrease as well as the result that equivalent width maxima are reached when the "bright" wave passes the systemic velocity are both in good agreement with the predictions of the model. Apart from these similarities there are two differences that are worth noting: first, the velocity range over which the variations occur is much smaller than the calculated one and second, the observed evolution of the modulations in time is rather smooth whereas the simulations yield rather abrupt and short-lived increases in intensity. These differences are important since they imply that the morphology of the perturbation we observed may depart from a pure spiral form. Summarising, we conclude that the wave-like "bright" modulation in the Hα profile can be due to an enhanced density perturbation that corotates with the star.

As far as the wave-like "dark" modulation is concerned, two alternative possibilities exist: either this modulation is due to absorption by spatially localised gas of very high density projected on the stellar core or it is due to weaker emission from regions of rarefied gas that corotate with the star. The former possibility seems rather unlikely since it confronts us with the necessity to explain how a gas volume that is projected on the stellar core can produce an absorption feature that moves from "blue" to "red" and back to "blue" within the profile. Thus we conclude that the wave-like "dark" modulation is likely due to emission from rarefied gas that corotates with the star. Unfortunately, the available observations do not allow us to go into detail and to discuss the position of the two perturbations with respect to each other. Nevertheless, it seems likely that the perturbations are not symmetric about the stellar center, otherwise one would be confronted with the problem that the second structure should be occulted by the disk when the first one crosses the line of sight (since Hα forms close to the star, $<1.3\,R_\star$), which is not seen in our observations. Thus we conclude that the deep-seated wind variability observed in α Cam in December–January 1999 can be qualitatively explained in terms of two rotationally modulated wind perturbations, the one of enhanced density and another of reduced density with respect to the mean, which are not symmetric about the center of the star. If this interpretation is correct, then it would imply that the inclination of the star with respect to the observer is $\sim$34° (as expected from the equality of $P_{\rm obs}$ and $P_{\rm rot}$).

One of the most intriguing feature of the rotationally modulated wind structure observed in December–January 1999 is that this structure was not stable: its lifetime is limited between $\sim$3 weeks to $\sim$6 months. The presence of large-scale time-dependent structures in the wind of α Cam was suggested by Kaper (1999) who observed systematic variations in Hα on a timescale of 5.6 days. Unfortunately, the author does not give any details concerning this result and thus does not allow us to judge whether or not the event observed by him is similar to the one we observed in December–January 1999. It is important to establish the lifetime and frequency of such wind structures in order to help determine their nature and origin.

Summarising, we conclude that the deep-seated wind activity of α Cam is rather complex and structures of quite different morphology are needed to interpret the results obtained in various epochs. It seems likely that most of the time the star is in a "normal" state in which

its wind activity is dominated by predominantly spherically symmetric mass loss variations. But during other times, for reasons unknown, the mass outflow becomes strongly asymmetric, giving rise to large-scale, but short-lived structures in the wind.

It seems likely that stellar pulsations might provide the seed perturbations for wind structure in α Cam. In particular, the ratio $(L/L_{\odot})/(M/M_{\odot})$ for this star is a factor of two larger than the $\sim 10^4$ lower limit, quoted by Glatzel (1999), above which strange-modes are predicted. This result implies that "strange-mode" instability could be the mechanism that generates perturbations at the base of the wind. The main advantage of this hypothesis is that it provides for the star to oscillate in radial and non-radial regimes and thus to generate large-scale wind structures of different geometry. Another possibility for the star to oscillate in a radial regime is radial fundamental pulsation. The adopted stellar parameters (Table 1) give for α Cam $P_{\rm fund} = 2.75$ days. This value is comparable to the timescale of wind variations in α Cam during its "normal" state. However, radial fundamental pulsations can hardly be reconciled with the idea of large-scale, asymmetric structures in the wind suggested to explain the December–January observations. To avoid this problem, one must assume that a mechanism, different from radial fundamental pulsation, is responsible for the generation of asymmetric mass outflow, e.g. short-lived "bright"/"cool" magnetic spots. Simultaneous spectral and photometric observations would be very helpful in testing various possibilities.

Acknowledgements. I would like to thank Dr. J. Puls for stimulating discussion. I am also grateful to the referee Dr. D. R. Gies for his valuable comments and suggestions which significantly improved the manuscript. I dedicate this paper to the memory of my friend and colleague Tashko Valchev who not only participated in the observations and did an enormous amount of work on the reduction of the data but also developed all program modules used in the present study. This work was supported by NSF to MES (Bulgaria) trough grant F-813/98 (N.M.)

References

Baade, D. 1992, in The atmosphere of early-type stars, ed. U. Heber, & C. S. Jeffery (Berlin: Springer), 145
Berghofer, T. W. 1999, Lect. Notes in Phys., 523, 203
Berghofer, T. W. , Baade, D., Schmitt, J. H. M. M., et al. 1996, A&A, 306, 899
Chalabaev, A., & Maillard, J. P. 1983, A&A, 127, 279
Cranmer, S. R., & Owocki, S. 1996, ApJ, 462, 469
Ebbets, D. 1982, ApJSS, 48, 399
Fullerton, A. W., Gies D. R., & Bolton C. T. 1996, ApJS, 103, 475
Gabler, R., Gabler, A., & Kudritzki, R.-P. 1989, A&A, 226, 162
Glatzel, W., Kiriakidis, M., Chemigovskij, S., et al. 1999, MNRAS, 303, 116
Harries, T. J. 2000, MNRAS, 315, 722
Howarth, I., & Prinja, R. 1989, ApJ, 69, 527
de Jager, C., Lamers, H. J. G. L. M., Macchetto, F., et al. 1979, A&A, 79, L28
de Jong, J. A., Henrichs, H. E., Schrijvers, C., et al. 1999, A&A, 345, 172
de Jong, J. A., Henrichs, H. F., Kaper, L. et al. 2001, A&A 368, 601
Kaper, L. 1999, Lect. Notes in Phys., 523, 193
Kaper, L., Henrichs, H. F., Nichols, J. S., et al. 1996, A&AS, 116, 237
Kaper, L., Henrichs, H. F., Fullerton, A. W., et al. 1997, A&A, 327, 281
Kaper, L., Henrichs, H. F., Nichols, J. S., & Telting, J. H. 1999, A&A, 344, 231
Kiriakidis, M., Fricke, K. J., & Glatzel, W. 1993, MNRAS, 264, 50
Lamers, H. J. G. L. M., Snow, Th., de Jager, C., & Langerwere, A. 1988, ApJ, 325, 342
Lennon, D. J., Dufton, P. L., & Fitzsimmmons, A. 1992, A&AS, 94, 569
Markova, N., & Valchev, T. 2000, A&A, 363, 995
Mullan, D. J, 1984, ApJ, 283, 303
Prinja, R. K. 1988, MNRAS, 231, 21
Prinja, R. K., & Howarth, I. D. 1986, ApJS, 61, 357
Prinja, R. K., Fullerton, A., & Crowther, P. A. 1996, A&A, 311, 264
Prinja, R. K., Stahl, O., Kaufer, A., et al. 2001, A&A, 367, 891
Puls J., Kudritzki, R.-P., Herrero, A., et al. 1996, A&A, 305, 171
Rauw, G., & Vreux, J.-M. 1998, A&A, 335, 995
Rauw, G., Morrison, N. D. Vreux, J.-M., et al. 2001, A&A, 366, 585
Reid A. H. N., & Howarth I. C. 1996, A&A, 311, 616
Roberts, D. H., Lehar, J., & Dreher, J. W. 1987, AJ, 93, 968
Scuderi, S., Bonanno, G., Di Benedetto, R., et al. 1992, ApJ, 392, 201
Stahl, O., Kaufer, A., Rivinius, Th., et al. 1996, A&A, 312, 539
Zeinalov, S. K., & Musaev, F. A. 1986, Sov. Astron. Lett., 12, 125